Parity violation in $\vec{\gamma} p$ Compton scattering

Jiunn-Wei Chen* and Thomas D. Cohen†
Department of Physics, University of Maryland, College Park, Maryland 20742-4111

Chung Wen Kao‡
Institut für Theoretische Physik, J. W. Goethe-Universität, D-60054 Frankfurt am Main, Germany
(Received 13 October 2000; published 24 October 2001)

Polarized beam $\vec{\gamma} p$ Compton scattering provides a theoretically clean way to extract the isovector parity violating pion-nucleon coupling constant $h_{\pi NN}^{(1)}$. This channel is more tractable experimentally than the recently proposed extraction of $h_{\pi NN}^{(1)}$ from the Bedaque-Savage process—polarized target $\gamma \vec{p}$ Compton scattering. The leading parity violating effect is calculated using heavy baryon chiral perturbation theory. The size of the asymmetry is estimated to be $\sim 4\times 10^{-8}$ for 120 MeV photon energy.

DOI: 10.1103/PhysRevC.64.055206 PACS number(s): 13.60.Fz, 14.20.Dh, 11.30.Er

The isovector parity violating (PV) pion-nucleon coupling constant $h_{\pi NN}^{(1)}$ is responsible for the longest range part of the $\Delta I=1$ PV NN forces [1–3]. It is expected to give dominant contributions to low energy quantities such as the nucleon[1] and nuclear anapole moment [6–11], and PV neutron radiative capture $\vec{n}p \to d\gamma$. However, past attempts to extract $h_{\pi NN}^{(1)}$ are not satisfactory (see [2,12,13] for reviews). In many-body systems, several PV effects are enhanced and have been detected. On the other hand, the theoretical analysis is complicated. The extractions from ^{18}F [14,15] and ^{133}Cs [16–19] systems differ by an order of magnitude with large uncertainties, while the measurement in the ^{205}Tl system gives a null result [20]. In fewer-body systems, the theory is more under control but the PV effect is smaller such that previous measurements could not reach the required precision [21–24]. However, there are several high precision new measurements under preparation or execution including $\vec{n}p \to d\gamma$ at LANSCE [25], $\vec{\gamma} d \to np$ at JLab [26], and the rotation of polarized neutrons in helium at NIST. It is expected that these experiments will put tight constraints on the value of $h_{\pi NN}^{(1)}$.

In the single nucleon system, a new PV observable was recently suggested by Bedaque and Savage [27]. They found that the polarized target $\gamma \vec{p} \to \gamma p$ Compton scattering asymmetry measurement (calculated to be $\sim 5\times 10^{-8}$ for 100 MeV photon energy) would determine $h_{\pi NN}^{(1)}$ with an estimated 15% uncertainty. To control systematic errors, the difference in cross section for the proton spin polarized parallel and antiparallel to the direction of the incident photon must be measured during a short period of time with only the target polarization direction changed. To achieve this, rapid flipping of the target polarization should be employed. This is impractical with the currently available experimental techniques and polarized proton targets; thus the Bedaque-Savage (BS) process is not favored experimentally. On the other hand, rapid flipping of beam helicity is a standard technique already employed in many parity violating experiments. Thus the polarized beam experiment $\vec{\gamma} p \to \gamma p$ is experimentally more tractable [32]. Given the great interest in the determination of $h_{\pi NN}^{(1)}$, we investigate this $\vec{\gamma} p$ parity violating process using heavy baryon chiral perturbation theory (HBχPT) [33,34].

We start by reviewing the symmetry constraints on the Compton scattering process

$$\gamma(k,\epsilon)+p \to \gamma(k',\epsilon')+p, \tag{1}$$

where (k,ϵ) and (k',ϵ') are the initial and final photon momenta and polarization vectors. It has been known for a long time that there are ten time reversal invariant structure functions in the transition amplitude for this process. Six of them conserve parity while four of them violate parity. This can be seen easily by the following exercise in helicity amplitude counting. Using $|\lambda_1,\lambda_2\rangle$ to denote a state with photon and proton helicity λ_1 and λ_2 in the center of mass frame, 16 helicity amplitudes $\langle \lambda_1',\lambda_2'|\lambda_1,\lambda_2\rangle$ can be constructed for proton Compton scattering. These amplitudes transform under time reversal as

$$\langle \lambda_1',\lambda_2'|\lambda_1,\lambda_2\rangle \xrightarrow{T} \langle \lambda_1,\lambda_2|\lambda_1',\lambda_2'\rangle, \tag{2}$$

which is equivalent to taking a transpose transformation of the 4×4 matrix. Thus ten time reversal invariant amplitudes can be constructed through the linear combination

$$\mathcal{M}_T(\lambda_1,\lambda_2,\lambda_1',\lambda_2') = \langle \lambda_1',\lambda_2'|\lambda_1,\lambda_2\rangle + \langle \lambda_1,\lambda_2|\lambda_1',\lambda_2'\rangle. \tag{3}$$

One can further separate these into parity conserving (PC) and PV amplitudes. Two of the amplitudes $\mathcal{M}_T(+1,+1/2,-1,-1/2)$ and $\mathcal{M}_T(+1,-1/2,-1,+1/2)$ have an additional symmetry. They are invariant under parity transformation,

*Electronic address: jwchen@physics.umd.edu
†Electronic address: cohen@physics.umd.edu
‡Electronic address: kaochung@th.physik.uni-frankfurt.de

[1]The isoscalar nucleon anapole moment is dominated by $h_{\pi NN}^{(1)}$, but not the isovector anapole moment which is more directly relevant for the SAMPLE electron-proton [4] and electron-deuteron [5] PV experiments.

$$\langle\lambda_1',\lambda_2'|\lambda_1,\lambda_2\rangle \xrightarrow{P} \langle -\lambda_1',-\lambda_2'|-\lambda_1,-\lambda_2\rangle, \tag{4}$$

after having been made to conserve time reversal invariance. The other eight amplitudes can be grouped into four PC and four PV amplitudes using similar linear combinations to that of Eq. (3). This demonstrates the well-known result that there are six independent PC and four independent PV structure functions satisfying time reversal invariance in a proton Compton scattering process.

In the center-of-mass frame, the six PC structure functions can be chosen as

$$\begin{aligned}T^{PC}=\bar{N}[&\mathcal{A}_1\epsilon\cdot\epsilon'^*+\mathcal{A}_2\hat{\mathbf{k}}\cdot\epsilon'^*\hat{\mathbf{k}}'\cdot\epsilon+i\mathcal{A}_3\sigma\cdot(\epsilon'^*\times\epsilon)\\&+i\mathcal{A}_4\sigma\cdot(\hat{\mathbf{k}}'\times\hat{\mathbf{k}})\epsilon\cdot\epsilon'^*+i\mathcal{A}_5\sigma\cdot[(\epsilon'^*\times\hat{\mathbf{k}})\epsilon\cdot\hat{\mathbf{k}}'\\&-(\epsilon\times\hat{\mathbf{k}}')\epsilon'^*\cdot\hat{\mathbf{k}}]+i\mathcal{A}_6\sigma\cdot[(\epsilon'^*\times\hat{\mathbf{k}}')\epsilon\cdot\hat{\mathbf{k}}'\\&-(\epsilon\times\hat{\mathbf{k}})\epsilon'^*\cdot\hat{\mathbf{k}}]]N,\end{aligned} \tag{5}$$

where N is the proton spinor, σ is the Pauli matrix acting on the nucleon spin index, $\hat{\mathbf{k}}$ and $\hat{\mathbf{k}}'$ are the unit vectors in the $\mathbf{k}$ and $\mathbf{k}'$ directions, and the Coulomb gauge ($\epsilon_0=\epsilon_0'=0$) is used. The PV structure functions can be chosen as

$$\begin{aligned}T^{PV}=\bar{N}[&\mathcal{F}_1\sigma\cdot(\hat{\mathbf{k}}+\hat{\mathbf{k}}')\epsilon\cdot\epsilon'^*-\mathcal{F}_2(\sigma\cdot\epsilon'^*\hat{\mathbf{k}}'\cdot\epsilon+\sigma\cdot\epsilon\hat{\mathbf{k}}\cdot\epsilon'^*)\\&-\mathcal{F}_3\hat{\mathbf{k}}\cdot\epsilon'^*\hat{\mathbf{k}}'\cdot\epsilon\sigma\cdot(\hat{\mathbf{k}}+\hat{\mathbf{k}}')-i\mathcal{F}_4\epsilon\times\epsilon'^*\cdot(\hat{\mathbf{k}}+\hat{\mathbf{k}}')]N.\end{aligned} \tag{6}$$

The $\mathcal{F}_{1-3}$ structures were first given in Ref. [27]. The interference between $\mathcal{A}_{1,2}$ and $\mathcal{F}_{1\text{-}3}$ contributes to the BS process. For the polarized beam process $\vec{\gamma}p\to\gamma p$ considered here, the contributions are from the interference between $\mathcal{A}_{1,2}$ and $\mathcal{F}_4$ and between $\mathcal{A}_{3\text{-}6}$ and $\mathcal{F}_{1\text{-}3}$.

Since we are interested in the low energy behavior of the proton Compton scattering process, chiral perturbation theory provides a natural framework with which to work. As a low energy effective field theory of QCD, chiral perturbation theory captures the symmetries of QCD and describes low energy observables by derivative and chiral expansions. The $SU(2)_L\times U(1)$ symmetry structure of electroweak interactions can also be incorporated with the weak boson exchange described by contact interactions while keeping the photon as dynamical degrees of freedom in the chiral Lagrangian.

HBχPT has been applied to the calculation of several Compton scattering observables. The PC structure functions have been calculated up to next-to-leading order (NLO), $\mathcal{O}(e^2p)$ [34], and are listed in the Appendix. The proton Thompson term is the only contribution at leading order (LO) and contributes to $\mathcal{A}_1$ only. The NLO contributions come from the tree level diagrams, pion-nucleon loop diagrams, and Wess-Zumino term. They contribute to all the PC structure functions $\mathcal{A}_{1\text{-}6}$ and contribute to the long distance part of the proton polarizabilities. Higher order effects, such as the proton recoil effect, the short distance contributions of proton polarizabilities, and the two-pion loop corrections, are neglected. Note that these structure functions can be determined experimentally (see the Appendix for more details); thus the uncertainty from the PC part can be eliminated completely. Here we use the HBχPT result only for the sake of estimation of the asymmetry. For the PV structure functions, the LO [$\mathcal{O}(G_Fe^2)$ with G_F the Fermi coupling constant] contributions have been calculated in Ref. [27]. We also list them in the Appendix. They arise from the pion loop diagrams shown in Fig. 1 and contribute to $\mathcal{F}_1$-$\mathcal{F}_3$. $\mathcal{F}_4$ is an additional quantity we will need to compute. Its contribution comes from the pion loop diagrams shown in Fig. 2 and the effect starts at NLO. Now we give some details of computing the $\mathcal{F}_4^{NLO}$.

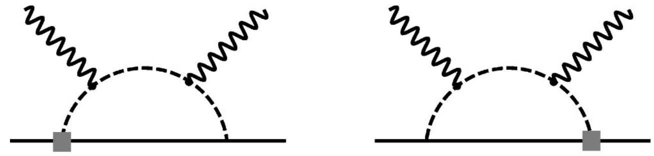

FIG. 1. The leading order contribution to parity violating structure functions $\mathcal{F}_1$–$\mathcal{F}_3$ in γp Compton scattering. The solid square is the weak operator with coefficient $h_{\pi NN}^{(1)}$. Wavy lines are photons, solid lines are nucleons, and dashed lines are pions. The crossed graphs are not shown. Graphs with photons from the strong vertex or insertion of the two-photon-pion vertex vanish in the $v\cdot A=0$ gauge, and thus are not shown here.

The PC part of the relevant Lagrangian is

$$\begin{aligned}\mathcal{L}^{PC}=&\frac{1}{2}D_\mu\pi_iD^\mu\pi_i-\frac{m_\pi^2}{2}\pi_i^2+i\bar{N}v_\mu D^\mu N\\&-\frac{g_A}{F_\pi}\bar{N}S_\mu(D^\mu\pi_i)\tau_iN+\frac{1}{2M_N}\bar{N}[(v\cdot D)^2-D^2]N\\&-\frac{ie}{M_N}\bar{N}[S^\mu,S^\nu][\mu_0+\mu_1\tau_3]NF_{\mu\nu}+\cdots,\end{aligned} \tag{7}$$

where the pion decay constant $F_\pi=93$ MeV, the pion-nucleon coupling constant $g_A=1.26$, N is the isospin doublet of the nucleon fields with velocity v, D is the covariant derivative with gauge coupling on the proton as $D_\mu N=(\partial-ieA)_\mu N$, and S is the covariant nucleon polarization vector. In the proton rest frame, $v^\mu=(1,0,0,0)$, $S^\mu=(0,\sigma/2)$. $\mu_0=(\mu_p+\mu_n)/2$ and $\mu_1=(\mu_p-\mu_n)/2$ are the isoscalar and isovector magnetic moments in nuclear magnetons, with $\mu_p=2.79$ and $\mu_n=-1.91$. The ellipsis denotes terms with more

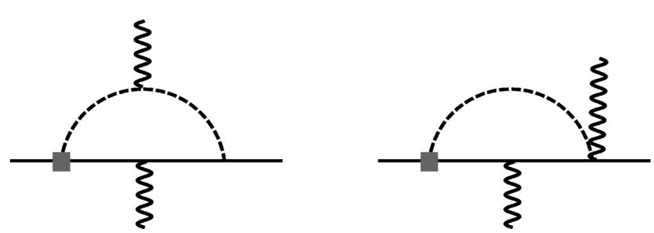

FIG. 2. The first nonvanishing order (NLO) contribution to parity violating structure functions $\mathcal{F}_4$ in γp Compton scattering. The features of the graphs are as defined in Fig. 1. The photon-nucleon couplings are magnetic couplings.

pion fields and insertions of higher powers of derivative and pion mass. Massive hadronic excitations such as kaons and deltas are ''integrated out.'' Their effects are encoded in the higher dimensional operators.

The nonleptonic PV part of the relevant Lagrangian is

$$\mathcal{L}^{PV}=\frac{h_{\pi NN}^{(1)}}{\sqrt{2}}\varepsilon^{3ij}\bar{N}\pi_i\tau_j N+\cdots=-ih_{\pi NN}^{(1)}\pi^+p^\dagger n+\text{H.c.}+\cdots, \tag{8}$$

where the ellipses denote terms with more pion fields and derivatives. This Lagrangian was first given in Ref. [3] with a different phase convention for the pion field. We adopt the same convention as Refs. [10,11]. $h_{\pi NN}^{(1)}$ was estimated by matching onto four-quark Fermi theory and was found to be dominated by s quark contributions,

$$|h_{\pi NN}^{(1)}|\sim\frac{G_F F_\pi \Lambda_\chi}{\sqrt{2}}\sim 5\times 10^{-7}, \tag{9}$$

where $\Lambda_\chi\sim 1$ GeV is the chiral perturbation scale. This estimation is consistent with the ''best value'' obtained in Ref. [1] and close to one result [28] from QCD sum rules. A recent calculation in the SU(3) Skyrme model yields $h_{\pi NN}^{(1)}\sim(0.8\text{–}1.3)\times 10^{-7}$ [29]. The radiative correction on the $h_{\pi NN}^{(1)}$ vertex is discussed in Ref. [30].

The $h_{\pi NN}^{(1)}$ term is the only term in $\mathcal{L}^{PV}$ with a nonderivative pion-nucleon coupling. It contributes to $\mathcal{F}_4$ through the pion loop diagrams in Fig. 2 and gives

$$\mathcal{F}_4^{NLO}=-\frac{e^2 g_A h_{\pi NN}^{(1)}\mu_n}{8\sqrt{2}m_N F_\pi \pi^2}\left[\omega-\frac{m_\pi^2}{\omega}\left(\sin^{-1}\frac{\omega}{m_\pi}\right)^2\right], \tag{10}$$

where the photon-nucleon coupling is magnetic. ω is the photon energy in the center-of-mass frame. Higher order PV operators involve more derivatives. There are only two PV operators [3] with one derivative that might contribute to $\mathcal{F}_4^{NLO}$. But the PV vector operator $\overline{p}v^\mu n D_\mu \pi^+$ can be removed by applying the equation of motion after integration by parts [31]. An explicit calculation to diagrams with this operator also gives a vanishing result. The PV axial vector operator $\overline{p}S^\mu p\pi^+ D_\mu \pi^-$ contribution depends on the proton polarization and thus does not contribute to $\mathcal{F}_4$. It gives corrections to $\mathcal{F}_{1-3}$ only at higher orders and can be neglected.

In this calculation delta contributions are encoded in the higher order operators and will contribute through higher order diagrams. If one considers the delta-nucleon mass difference $\Delta\sim 300$ MeV as a light scale as m_π and ω are, then one needs to sum factors of m_π/Δ and ω/Δ to all orders. This can be done by including delta as a dynamical degree of freedom [33,35]. In this expansion, the delta diagrams will contribute to $\mathcal{F}_{1-4}^{NLO}$ through $\pi\Delta$ loop diagrams and tree diagrams with unknown $\gamma N\Delta$ couplings. In the expansion with which we work, the Δ is considered as a large or heavy scale, so factors of m_π/Δ and ω/Δ are treated perturbatively. Thus below the pion production threshold ($\omega<m_\pi$) the delta contributes a factor of $(m_\pi^2/\Delta^2,\omega^2/\Delta^2)\sim 25\%$ correction to $\mathcal{F}_4^{NLO}$. This is the dominant source of the uncertainty.

The PV asymmetry can be defined by the difference in the cross section (in the center-of-mass frame) for photon helicity $\lambda_\gamma=+1$ and -1 normalized to the sum

$$A_{\gamma\gamma}(\omega,\theta)\equiv\frac{(d\sigma/d\Omega)(\lambda_\gamma=+1)-(d\sigma/d\Omega)(\lambda_\gamma=-1)}{(d\sigma/d\Omega)(\lambda_\gamma=+1)+(d\sigma/d\Omega)(\lambda_\gamma=-1)}. \tag{11}$$

Again, the PC structure functions $\mathcal{A}_{1-6}$ can be extracted from experiments to further reduce theoretical input and eliminate the uncertainties from the PC part. Here we insert the PC HBχPT result in order to get an estimation of the size of the asymmetry. In this treatment, the helicity asymmetry contribution starts at NLO,

$$\begin{aligned}A_{\gamma\gamma}(\omega,\theta)=&\frac{2\sin^2\theta}{|\mathcal{A}_1^{LO}|^2(1+\cos^2\theta)}\text{Re}\{\mathcal{A}_1^{LO}\mathcal{F}_4^{NLO*}+\mathcal{A}_3^{NLO}[\mathcal{F}_1^{LO*}-2\mathcal{F}_2^{LO*}-\mathcal{F}_3^{LO*}(1+\cos\theta)]\\&+\mathcal{A}_5^{NLO}[\mathcal{F}_1^{LO*}(1+\cos\theta)+\mathcal{F}_2^{LO*}(1-3\cos\theta)+\mathcal{F}_3^{LO*}(1-\cos^2\theta)]\\&-\mathcal{A}_6^{NLO}[\mathcal{F}_1^{LO*}(1+\cos\theta)+\mathcal{F}_2^{LO*}(3-\cos\theta)+\mathcal{F}_3^{LO*}(1-\cos^2\theta)]-\mathcal{A}_4^{NLO}\mathcal{F}_2^{LO*}(1+\cos\theta)\}\\&-\frac{4(1+\cos\theta)}{|\mathcal{A}_1^{LO}|^2(1+\cos^2\theta)}\text{Re}\{\mathcal{A}_3^{NLO}\mathcal{F}_1^{LO*}+\mathcal{A}_1^{LO}\mathcal{F}_4^{NLO*}\}.\end{aligned} \tag{12}$$

We have used the LO result for the PC cross section, so

$$\frac{1}{2}\left[\frac{d\sigma}{d\Omega}(\lambda_\gamma=+1)+\frac{d\sigma}{d\Omega}(\lambda_\gamma=-1)\right]=\frac{1}{2(4\pi)^2}|\mathcal{A}_1^{LO}|^2(1+\cos^2\theta)=\frac{\alpha^2}{2M_N^2}(1+\cos^2\theta). \tag{13}$$

It is instructive to study the low energy limit ($\omega\ll m_\pi$) of the asymmetry. Keeping the first term in the ω/m_π expansion,

$$\mathcal{A}_1^{LO} = -\frac{e^2}{M_N}, \quad \mathcal{A}_3^{NLO} \sim [1+2\kappa_p-(1+\kappa_p)^2\cos\theta]\frac{e^2\omega}{2M_N^2}, \quad \mathcal{A}_4^{NLO} = -\mathcal{A}_5^{NLO} \sim -\frac{(1+\kappa_p)^2 e^2\omega}{2M_N^2},$$

$$\mathcal{A}_6^{NLO} \sim -\frac{(1+\kappa_p)e^2\omega}{2M_N^2}, \quad \mathcal{F}_1^{LO*} = \mathcal{F}_2^{LO*} \sim -\frac{e^2 g_A h_{\pi NN}^{(1)}\omega^2}{24\sqrt{2}\pi^2 F_\pi m_\pi^2}, \quad \mathcal{F}_4^{NLO*} \sim +\frac{e^2 g_A h_{\pi NN}^{(1)}\mu_n\omega^3}{24\sqrt{2}\pi^2 F_\pi M_N m_\pi^2}, \tag{14}$$

with $\mathcal{F}_3^{LO*} = O(\omega^4/m_\pi^4)$ and $\kappa_p \equiv \mu_p - 1$. The inverse power of m_π dependence in the $\mathcal{F}$'s explains why there are no intrinsic unknown two-photon–two-nucleon counterterms at this order. In this low energy limit, the asymmetry has a simple form,

$$A_{\gamma\gamma}(\omega \ll m_\pi, \theta) = -\frac{g_A h_{\pi NN}^{(1)}\{[2\mu_n+(\mu_p+1)^2]\sin^2\theta - 2(1+\cos\theta)[2\mu_n-(\mu_p-1)^2]\}\omega^3}{24\sqrt{2}\pi^2 F_\pi m_\pi^2(1+\cos^2\theta)}\left[1+\mathcal{O}\left(\frac{\omega^2}{m_\pi^2}, \frac{m_\pi^2}{\Delta^2}\right)\right]. \tag{15}$$

The vanishing of $A_{\gamma\gamma}$ at backward angles ($\theta = \pi$) is a consequence of time reversal invariance and is a general property for all values of the photon energy. For backscattering, the change of photon spin direction corresponds to a $\Delta J = 2$ operation and hence is a forbidden transition for the proton matrix element. Thus neither photon nor proton spin direction changes but the helicities change signs. Using Eq. (3) for the time reversal invariant amplitude and $(\lambda_1', \lambda_2') = (-\lambda_1, -\lambda_2)$, this amplitude conserves parity and does not contribute to the PV asymmetry.

For a numerical estimation of the magnitude of the asymmetry, we consider $\theta = \pi/2$, where

$$A_{\gamma\gamma}\left(\omega \ll m_\pi, \frac{\pi}{2}\right) \sim -8.8\times 10^{-9}\left(\frac{h_{\pi NN}^{(1)}}{5\times 10^{-7}}\right)\left(\frac{\omega}{70\ \text{MeV}}\right)^3 \tag{16}$$

with $\sim 25\%$ uncertainty.

In Fig. 3, we show the photon energy dependence of the estimated asymmetry at $\theta = \pi/2$. Assuming the naive size for $h_{\pi NN}^{(1)}$ estimated in Eq. (9), the asymmetry is $A_{\gamma\gamma}(120\ \text{MeV}, \pi/2) \sim -3.8\times 10^{-8}$, with the higher order uncertainty $\sim (m_\pi^2/\Delta^2, \omega^2/\Delta^2) \sim 25\%$. Note that very near the pion production threshold, resummation of terms with powers of

$$\frac{m_\pi^2}{2m_N(\omega - m_\pi)} \tag{17}$$

is required in order to shift the pion production threshold from m_π to $m_\pi + m_\pi^2/2m_N$ (in the laboratory frame) to recover the recoil effect. The resummation procedure is well known [36]. Without this resummation, we should restrict ourselves to $\omega < 130$ MeV such that the factor in Eq. (17) is sufficiently less than 1. To probe how far away from the threshold our calculation is still under control, we compare the result of expanding the $A_{\gamma\gamma}$ to NLO to that of expanding the total amplitude to NLO, then squaring it to get the $A_{\gamma\gamma}$ (the $\mathcal{A}_2$-$\mathcal{F}_4$ interference term is included in the latter case). If the difference between these two quantities is consistent with the estimated higher order contribution, then the result without extra resummation will be valid. We find the difference increases with ω and reaches 14% at $\omega = 120$ MeV, so our expansion is presumably still useful up to 120 MeV.

In Fig. 4, we show the angular distribution at $\omega = 120$ MeV for the same estimated value of $h_{\pi NN}^{(1)}$. The maximum asymmetry is near $\theta = \pi/2$ but slightly biased toward the forward direction. The asymmetry vanishes at $\theta = \pi$ as required by time reversal invariance.

In conclusion, parity violating $\vec{\gamma} p \to \gamma p$ Compton scattering provides a theoretically clean way to extract $h_{\pi NN}^{(1)}$. The dominating source of the PV effect comes from the PV pion loop contributions. The magnitude of the helicity asymmetry

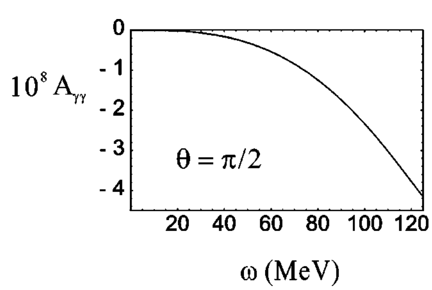

FIG. 3. The estimated photon helicity asymmetry $A_{\gamma\gamma}$ defined in Eq. (11) shown as a function of photon energy with the photon reflection angle $\theta = \pi/2$ in the center-of-mass frame. The naively estimated value of $h_{\pi NN}^{(1)} = 5\times 10^{-7}$ is taken as input, and a HBχPT estimation used for the parity conserving amplitude.

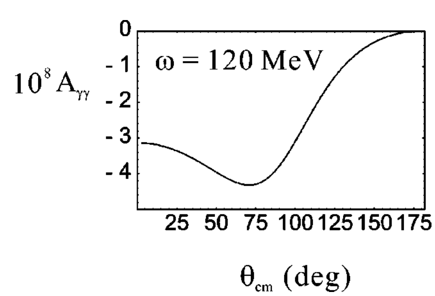

FIG. 4. The angular distribution of the estimated photon helicity asymmetry $A_{\gamma\gamma}$ defined in Eq. (11) and calculated in HBχPT in the center-of-mass frame for 120 MeV photon energy. The naively estimated value of $h_{\pi NN}^{(1)} = 5\times 10^{-7}$ is taken as input.

is estimated to be $\sim 4\times 10^{-8}$ at 120 MeV photon energy with $\sim$25% uncertainty for a natural size $h^{(1)}_{\pi NN}$, under the framework of HBχPT. Thus we have found a model independent way to constrain $h^{(1)}_{\pi NN}$ with $\sim$25% uncertainty. We note that the $\sim$25% uncertainty is predominantly due to the delta and can in principle be reduced by inclusion of the delta as an explicit degree of freedom. Unfortunately this would require additional experiments to measure the PV $\gamma N\Delta$ coupling. However, even with $\sim$25% uncertainties, $\vec{\gamma}p$ Compton scattering will greatly improve our understanding of $h^{(1)}_{\pi NN}$. We are optimistic that this experiment is feasible for current experimental techniques and facilities.

ACKNOWLEDGMENTS

J.W.C. and T.D.C. thank the Institute for Nuclear Theory at the University of Washington for its hospitality and the U.S. Department of Energy for partial support during the completion of this work. J.W.C. thanks P. Bedaque, T. Hemmert, X. Ji, U. Meissner, M. Ramsey-Musolf, M. Savage, R. Springer, and R. Suleiman for useful discussions. J.W.C. and T.D.C. were supported in part by the U.S. Department of Energy under Grant No. DE-FG02-93ER-40762. C.W.K was supported by the Alexander von Humboldt Foundation.

APPENDIX

The following PC structure functions computed to $\mathcal{O}(e^2p)$ are taken from Eqs. (4.28a–g) of Ref. [34] [with a typo in Eq. (4.28b) corrected]:

$$\mathcal{A}_1^{LO}=-\frac{e^2}{M_N},$$

$$\mathcal{A}_1^{NLO}=\frac{g_A^2e^2}{8\pi F_\pi^2}\left\{m_\pi-\sqrt{m_\pi^2-\omega^2}+\frac{2M_\pi^2-t}{\sqrt{-t}}\times\left[\frac{1}{2}\arctan\frac{\sqrt{-t}}{2m_\pi}-\int_0^1 dz\arctan\frac{(1-z)\sqrt{-t}}{2\sqrt{M_\pi^2-\omega^2z^2}}\right]\right\}, \tag{A1}$$

$$\mathcal{A}_2^{NLO}=\frac{e^2\omega}{M_N^2}+\frac{e^2g_A^2\omega^2}{8\pi F_\pi^2}\frac{t-2m_\pi^2}{(-t)^{3/2}}\int_0^1 dz\left[\arctan\frac{(1-z)\sqrt{-t}}{2\sqrt{m_\pi^2-\omega^2z^2}}-\frac{2(1-z)\sqrt{t(\omega^2z^2-m_\pi^2)}}{4m_\pi^2-4\omega^2z^2-t(1-z)^2}\right], \tag{A2}$$

$$\mathcal{A}_3^{NLO}=\frac{e^2\omega}{2M_N^2}[1+2\kappa_p-(1+\kappa_p)^2\cos\theta]+\frac{e^2g_At\omega}{8\pi^2F_\pi^2(m_\pi^2-t)}+\frac{e^2g_A^2}{8\pi^2F_\pi^2}\left[\frac{M_\pi^2}{\omega}\arcsin^2\frac{\omega}{m_\pi}-\omega\right]+\frac{e^2g_A^2}{4\pi^2F_\pi^2}\omega^4\sin^2\theta\int_0^1dx\int_0^1dz\frac{x(1-x)z(1-z)^3}{W^3}\times\left[\arcsin\frac{\omega z}{R}+\frac{\omega zW}{R^2}\right], \tag{A3}$$

$$\mathcal{A}_4^{NLO}=-\frac{e^2(1+\kappa_p)^2\omega}{2M_N^2}+\frac{e^2g_A^2}{4\pi^2F_\pi^2}\int_0^1dx\int_0^1dz\frac{z(1-z)}{W}\arcsin\frac{\omega z}{R}, \tag{A4}$$

$$\mathcal{A}_5^{NLO}=\frac{e^2\omega}{2M_N^2}(1+\kappa_p)^2-\frac{e^2g_A\omega^3}{8\pi^2F_\pi^2(m_\pi^2-t)}+\frac{e^2g_A^2\omega^2}{8\pi^2F_\pi^2}\int_0^1dx\int_0^1dz\left[-\frac{(1-z)^2}{W}\arcsin\frac{\omega z}{R}+2\omega^2\cos\theta\frac{x(1-x)z(1-z)^3}{W^3}\times\left(\arcsin\frac{\omega z}{R}+\frac{\omega zW}{R^2}\right)\right], \tag{A5}$$

$$\mathcal{A}_6^{NLO}=-\frac{e^2\omega}{2M_N^2}(1+\kappa_p)+\frac{e^2g_A\omega^3}{8\pi^2F_\pi^2(m_\pi^2-t)}+\frac{e^2g_A^2\omega^2}{8\pi^2F_\pi^2}\int_0^1dx\int_0^1dz\left[\frac{(1-z)^2}{W}\arcsin\frac{\omega z}{R}-2\omega^2\frac{x(1-x)z(1-z)^3}{W^3}\left(\arcsin\frac{\omega z}{R}+\frac{\omega zW}{R^2}\right)\right], \tag{A6}$$

with

$$t=(k-k')^2=-2\omega^2(1-\cos\theta),$$

$$W=\sqrt{m_\pi^2-\omega^2z^2+t(1-z)^2x(x-1)},$$

$$R=\sqrt{m_\pi^2+t(1-z)^2x(x-1)}. \tag{A7}$$

Expressions of PC Compton scattering for the unpolarized differential cross section $d\sigma/d\Omega$, proton-photon spin parallel asymmetry $\mathcal{A}_\parallel$, and proton-photon spin perpendicular asymmetry $\mathcal{A}_\perp$ are given in terms of PC structure functions in Eqs. (4.18) and (4.19) of Ref. [34]. These structure functions can be extracted experimentally. For example, below the pion production threshold ($\omega<m_\pi$), one can extract $\mathcal{A}_1$ and $\mathcal{A}_3$ by measuring $d\sigma/d\Omega$ and $\mathcal{A}_\parallel$ at $\theta=0$. Since $\mathcal{A}_i$ are all real below pion production threshold and $\mathcal{A}_\parallel\propto\mathcal{A}_1^2+\mathcal{A}_3^2$ and $\mathcal{A}_\perp\propto\mathcal{A}_1\mathcal{A}_3$, measurements of $\mathcal{A}_\parallel$ and $\mathcal{A}_\perp$ are sufficient to extract $\mathcal{A}_1$ and $\mathcal{A}_3$.

The following PV structure functions are given by Ref. [27]:

$$\mathcal{F}_1(\omega,\theta)=\frac{e^2 g_A h^{(1)}_{\pi NN}}{4\sqrt{2}\pi^2 F_\pi}\int_0^1 dx\int_0^{1-x} dy(1-2y)$$
$$\times\omega[\mathcal{I}(-1;x\omega,\widetilde{m}^2)-\mathcal{I}(-1;-x\omega,\widetilde{m}^2)],$$

$$\mathcal{F}_2(\omega,\theta)=\frac{e^2 g_A h^{(1)}_{\pi NN}}{2\sqrt{2}\pi^2 F_\pi}\int_0^1 dx\int_0^{1-x} dy\, y\,\omega[\mathcal{I}(-1;x\omega,\widetilde{m}^2)$$
$$-\mathcal{I}(-1;-x\omega,\widetilde{m}^2)],$$

$$\mathcal{F}_3(\omega,\theta)=\frac{e^2 g_A h^{(1)}_{\pi NN}}{2\sqrt{2}\pi^2 F_\pi}\int_0^1 dx\int_0^{1-x} dy\, y(1-x-y)(2y-1)$$
$$\times\omega^3[\mathcal{I}(-2;x\omega,\widetilde{m}^2)-\mathcal{I}(-2;-x\omega,\widetilde{m}^2)],$$

$$\widetilde{m}^2=m_\pi^2+2y(1-x-y)\omega^2(1-\cos\theta), \tag{A8}$$

where the functions $\mathcal{I}(\alpha;b,c)$ are defined by Jenkins and Manohar in Ref. [33]:

$$\mathcal{I}(\alpha;b,c)=\int_0^\infty d\lambda(\lambda^2+2\lambda b+c)^\alpha,$$

$$\mathcal{I}(-1;\Delta,m^2)=-\frac{1}{2\sqrt{\Delta^2-m^2+i\epsilon}}\log\left(\frac{\Delta-\sqrt{\Delta^2-m^2+i\epsilon}}{\Delta+\sqrt{\Delta^2-m^2+i\epsilon}}\right),$$

$$\mathcal{I}(-2;\Delta,m^2)=\frac{1}{2(\Delta^2-m^2+i\epsilon)}\left(\frac{\Delta}{m^2}-\mathcal{I}(-1;\Delta,m^2)\right). \tag{A9}$$

[1] B. Desplanques, J. F. Donoghue, and B. R. Holstein, Ann. Phys. (N.Y.) **124**, 449 (1980).
[2] E. G. Adelberger and W. C. Haxton, Annu. Rev. Nucl. Part. Sci. **35**, 501 (1985).
[3] D. B. Kaplan and M. J. Savage, Nucl. Phys. **A556**, 653 (1993).
[4] SAMPLE Collaboration, D. T. Spayde *et al.*, Phys. Rev. Lett. **84**, 1106 (2000).
[5] Bates experiment No. 94-11, M. Pitt and E.J. Beise, contacts; M. Pitt and E.J. Beise (private communication).
[6] Y. B. Zel'dovich, Sov. Phys. JETP **6**, 1184 (1958); **12**, 777 (1961).
[7] W. C. Haxton, E. M. Henley, and M. J. Musolf, Phys. Rev. Lett. **63**, 949 (1989).
[8] M. J. Musolf and B. R. Holstein, Phys. Rev. D **43**, 2956 (1991).
[9] M. J. Savage and R. P. Springer, Nucl. Phys. **A644**, 635 (1998); **A657**, 457(E) (1999); nucl-th/9907069.
[10] C. M. Maekawa and U. van Kolck, Phys. Lett. B **478**, 73 (2000); C. M. Maekawa, J. S. Veiga, and U. van Kolck, *ibid.* **488**, 167 (2000).
[11] S.-L. Zhu, S. J. Puglia, B. R. Holstein, and M. J. Ramsey-Musolf, Phys. Rev. D **62**, 033008 (2000).
[12] W. Haeberli and B. R. Holstein, in *Symmetries and Fundamental Interactions in Nuclei*, edited by W. C. Haxton and E. M. Henley (World Scientific, Singapore, 1995), p. 17.
[13] W. T. H. van Oers, Int. J. Mod. Phys. E **8**, 417 (1999); hep-ph/9910328.
[14] S. A. Page *et al.*, Phys. Rev. C **35**, 1119 (1987).
[15] M. Bini, T. F. Fazzini, G. Poggi, and N. Taccetti, Phys. Rev. C **38**, 1195 (1988).
[16] C. S. Wood *et al.*, Science **275**, 1759 (1997).
[17] W. C. Haxton, Science **275**, 1753 (1997).
[18] V. V. Flambaum and D. W. Murray, Phys. Rev. C **56**, 1641 (1997).
[19] W. S. Wilburn and J. D. Bowman, Phys. Rev. C **57**, 3425 (1998).
[20] P. A. Vetter *et al.*, Phys. Rev. Lett. **74**, 2658 (1995).
[21] V. A. Knyazkov *et al.*, Nucl. Phys. **A417**, 209 (1984).
[22] J. F. Cavagnac, B. Vignon, and R. Wilson, Phys. Lett. B **367**, 138 (1997); J. Alberi *et al.*, in *Proceedings of the Symposium/Workshop on Spin and Symmetries*, edited by W. D. Ramsay and W. T. H. van Oers [Can. J. Phys. **66**, 542 (1988)].
[23] E. D. Earle *et al.*, in *Proceedings of the Symposium/Workshop on Spin and Symmetries*, edited by W. D. Ramsay and W. T. H. van Oers [Can. J. Phys. **66**, 534 (1988)].
[24] D. M. Markoff, Ph.D. thesis, University of Washington, 1997.
[25] W. M. Snow *et al.*, Nucl. Instrum. Methods Phys. Res. A **440**, 729 (2000).
[26] JLab LOI 00-002, W. van Oers and B. Wojtsekhowski, contacts.
[27] P. F. Bedaque and M. J. Savage, Phys. Rev. C **62**, 018501 (2000).
[28] E. M. Henley, W.-Y. P. Hwang, and L. S. Kisslinger, Phys. Lett. B **367**, 21 (1999); **440**, 449(E) (1998).
[29] U. G. Meissner and H. Weigel, Phys. Lett. B **447**, 1 (1999).
[30] S.-L. Zhu, S. J. Puglia, B. R. Holstein, and M. J. Ramsey-Musolf, hep-ph/0008140.
[31] J. W. Chen and X. Ji, hep-ph/0101290.
[32] R. Suleiman (private communication).
[33] E. Jenkins and A. V. Manohar, Phys. Lett. B **255**, 558 (1991).
[34] V. Bernard, N. Kaiser, and Ulf-G. Meissner, Int. J. Mod. Phys. E **4**, 193 (1995).
[35] T. R. Hemmert, B. R. Holstein, and J. Kambor, Phys. Lett. B **395**, 89 (1997).
[36] T. Becher and H. Leutwyler, Eur. Phys. J. C **9**, 643 (1999).